

Valence transitions in the heavy-fermion compound YbCuAl as a function of temperature and pressure

Hitoshi Yamaoka,¹ Naohito Tsujii,² Yuki Utsumi,³ Hitoshi Sato,⁴ Ignace Jarrige,⁵ Yoshiya Yamamoto,⁶ Jung-Fu Lin,⁷ Nozomu Hiraoka,⁸ Hirofumi Ishii,⁸ Ku-Ding Tsuei,⁸ and Jun'ichiro Mizuki^{6,9}

¹RIKEN/SPring-8, Sayo, Hyogo 679-5148, Japan

²Quantum Beam Center, National Institute for Materials Science, 1-2-1 Sengen, Tsukuba 305-0047, Japan

³Graduate School of Science, Hiroshima University, Higashi-Hiroshima 739-8526, Japan

⁴Hiroshima Synchrotron Radiation Center, Hiroshima University, Higashi-Hiroshima 739-0046, Japan

⁵National Synchrotron Light Source II, Brookhaven National Laboratory, Upton, New York 11973, USA

⁶Graduate School of Science and Technology, Kwansai Gakuin University, Sanda, Hyogo 669-1337, Japan

⁷Department of Geological Sciences, The University of Texas at Austin, Austin, Texas 78712, USA

⁸National Synchrotron Radiation Research Center, Hsinchu 30076, Taiwan

⁹Japan Atomic Energy Agency, SPring-8, Sayo, Hyogo 679-5148, Japan

(Received 1 February 2013; revised manuscript received 14 April 2013; published 13 May 2013)

We report on direct measurements of the Yb valence in the heavy Fermion compound YbCuAl as a function of temperature and pressure using resonant x-ray emission spectroscopy. The increase of the Yb²⁺ component at $T < 100$ K and ambient pressure, well described by the single impurity Anderson model, is found to compensate for the thermal contraction of the unit cell volume. Under pressure, the Yb valence increases continuously up to 25 GPa, albeit a marked leveling off close to the critical pressure, at $P \geq 13$ GPa. This finding is reminiscent of a recent report on YbCu₂Si₂ and further confirms the interplay between electronic and magnetic fluctuations near the magnetic instability point of rare-earth intermediate-valence materials.

DOI: [10.1103/PhysRevB.87.205120](https://doi.org/10.1103/PhysRevB.87.205120)

PACS number(s): 71.27.+a, 71.28.+d, 75.30.Mb, 78.70.En

I. INTRODUCTION

Quantum criticality in $4f$ -based heavy fermion systems is a central problem in condensed-matter physics, because it can cause remarkable emergent properties such as non-Fermi-liquid behavior and unconventional superconductivity. Quantum criticality arises from the interplay between the Ruderman-Kittel-Kasuya-Yosida (RKKY) interaction between the $4f$ electrons mediated by hybridized conduction electrons and the Kondo screening of the $4f$ moments by the conduction electrons.¹⁻³ The Kondo temperature, or the c - f hybridization strength, can be affected by an external parameter such as external pressure, allowing one to probe the behavior of a system in the vicinity of a quantum critical point (QCP).

The symmetry in the pressure dependence of the c - f hybridization strength between Ce and Yb-based materials arising from the electron-hole symmetry of the Ce and Yb $4f$ shell is of particular interest. The electron-hole symmetry results in admirably symmetric pressure-dependent physical properties, such as pressure-induced transitions from antiferromagnetic ordering to mixed valence via the QCP for Ce systems and the reverse transitions for Yb systems. Recently, however, the possibility of unsymmetrical behaviors for Ce and Yb systems has been suggested—Goltsev *et al.*⁴ pointed out that some Yb compounds can undergo a reentrance transition to a mixed-valent state at high pressure that is beyond the pressure-induced magnetic ordered phase for the trivalent state. YbCu₂Si₂ has been considered as a candidate compound for such an anomaly because its maximum temperature of the resistivity T_{\max} shows a minimum at $P = 15$ GPa, in which T_{\max} increases with pressure. This behavior was attributed to the increase of the Kondo temperature (T_K) as a function of pressure due to the enhancement of c - f hybridization.

However, direct measurements of the Yb valence in YbCu₂Si₂ have been recently conducted at low temperature and high pressure. These results showed a characteristic kink around the QCP in the slope of Yb valence versus pressure, but no indication of a reentrant valence transition was observed up to 20 GPa.⁵

Here we examined the possibility of a valence reentrance at high pressures using the candidate, archetypal heavy fermion, YbCuAl. In an early report by Mignot and Wittig,⁶ high-pressure resistivity of the system at room temperature was shown to exhibit a minimum around 8 GPa, followed by a gradual increase up to 20 GPa. If this is an indication of an increase in the Kondo scattering, i.e., of T_K , pressure-dependent measurements for the strength of the c - f hybridization or the valence are highly desired. So far, conflicting information about the pressure dependence of the Yb valence in YbCuAl has been reported. The quadrupole coupling in Mössbauer spectroscopy indicated that a valence transition towards Yb³⁺ was completed at approximately 5 GPa,⁷ whereas signs of magnetic ordering transition to the trivalent state were suggested using resistivity results at 1 K and 8 GPa.⁸ This mismatch between the electronic and magnetic transitions remains unsolved, and further calls for a reliable study of the Yb $4f$ electronic occupancy as a function of pressure.

In this paper we present experimental results on the Yb valence in YbCuAl as a function of temperature as low as 8 K and pressure up to 25 GPa by employing bulk-sensitive techniques to probe its electronic structures, including partial fluorescence yield x-ray absorption spectroscopy (PFY-XAS) and resonant x-ray emission spectroscopy (RXES). We have observed that the valence increases steadily with pressure until around 13 GPa, and then levels off at higher pressures. This change in the slope in the valence manifests a possible change in the magnetic fluctuations, indicating the occurrence of a

magnetic instability point.⁵ While the valence is still slightly below 3 at 25 GPa, Yb adopts the magnetic trivalent state when the valence reaches ~ 2.95 at 8 GPa. However, no evidence of a reentrant valence transition was found up to 25 GPa.

II. EXPERIMENTS

A polycrystalline sample of YbCuAl was prepared in a closed tantalum tube filled with argon by a high-frequency induction furnace and then annealed. YbCuAl exhibits the Fe₂P-type hexagonal crystal structure [see Fig. 1(c)] with the space group $P62m$.⁹ Magnetic susceptibility of the sample was measured with a superconducting quantum interference device (SQUID) magnetometer at an applied field of 1000 Oe. The temperature dependence of the lattice constants was measured down to 10 K using a Rigaku RINT2000 x-ray diffractometer.

PFY-XAS and RXES measurements were performed at the Taiwan Beamline BL12XU, SPring-8.¹⁰⁻¹³ The undulator beam was monochromatized by a pair of cryogenically cooled Si(111) crystals and focused to a size of 15(horizontal) \times 30(vertical) μm^2 at the sample position using toroidal and Kirkpatrick-Baez mirrors. Incident photon flux was estimated to be about 9×10^{12} photons/s at 8.94 keV measured by a pin diode (type S3590-09). A Johann-type spectrometer equipped with a spherically bent Si(620) crystal (radius of ~ 1 m) was used to analyze the Yb emission of $3d_{5/2} \rightarrow 2p_{3/2}$ deexcitation

following a $2p_{3/2} \rightarrow 5d$ excitation with a solid state detector (XFlash 1001 type 1201). The overall energy resolution was estimated to be about 1 eV at the emitted photon energy of 7400 eV for the elastic scattering. The intensities of all sample spectra are normalized by the intensity of the incident beam that was monitored by an ion chamber just before the sample.

A closed-circuit He cryostat was used for temperature-dependent measurements as low as 8 K at the beamline BL12XU at SPring-8. High-pressure conditions were achieved using a diamond anvil cell coupled with a gas membrane. A Be gasket 2 mm in diameter and approximately 100 μm thick preindented to approximately 40 μm thick. The diameter of the sample chamber in the gasket was approximately 150 μm and the diamond anvil culet size was 400 μm . We used the Be gasket in-plane geometry where both incoming and outgoing x-ray beams passed through the Be gasket due to its higher transmissivity to the x rays in comparison to other high-Z materials. Pressures of the sample chamber were monitored using the ruby R_1 line fluorescence.

III. RESULTS AND ANALYSES

A. Magnetic susceptibility

The temperature dependence of the magnetic susceptibility χ of YbCuAl is shown in Figs. 1(a) and 1(b). χ decreases at

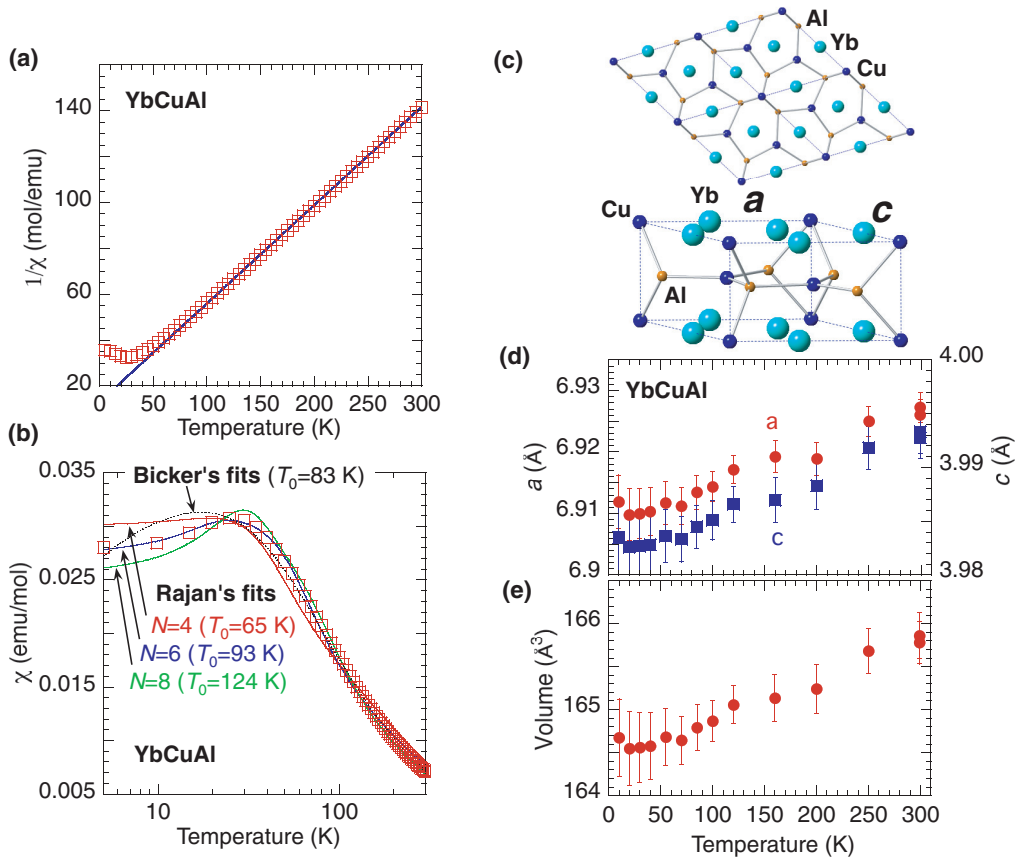


FIG. 1. (Color online) (a) Inverse of the magnetic susceptibility (open squares) as a function of temperature with the Curie-Weiss fit at $T > 150$ K. (b) Magnetic susceptibility (open squares) and fits based on the single impurity Anderson models.^{14,15} Estimated characteristic temperatures (T_0) are also indicated. (c) Crystal structure. (d) Lattice constants a and c as a function of temperature. (e) Volume as a function of temperature.

temperatures above $T \sim 30$ K. We fitted the $1/\chi$ curve with the formula $1/\chi = (T - \Theta_p)/C$ at $T \geq 150$ K as shown in Fig. 1(a), where Θ_p and C are the Weiss temperature and the Curie constant, respectively. We obtained $C = 2.33$ and $\Theta_p = -29.7$ K. The Curie constant is expressed as $C = N_A \mu_{\text{eff}}^2 / 3k_B$, where μ_{eff} , N_A , and k_B are the effective magnetic moment, Avogadro's number, and Boltzmann's constant, respectively. In the Yb systems, where valence fluctuations are expected, the effective magnetic moment can be used as a measure of the degree of the valence admixture since the Yb^{3+} ($4f^{13}$, $J = 7/2$) ion displays a magnetic moment while the Yb^{2+} ($4f^{14}$, $J = 0$) is nonmagnetic. μ_{eff} is estimated to be $4.32 \mu_B$, which is slightly smaller than $4.54 \mu_B$ for Yb^{3+} ion which was calculated using the formula according to Hund's rule $\mu_{\text{eff}} = g\sqrt{J(J+1)}\mu_B$, where g is the Landé g factor. The effective magnetic moment indicates that Yb is nearly trivalent with a small fraction of the divalent component.

According to the Bethe-Ansatz solution of the Coqblin-Schrieffer model based on the SIAM, the physical properties of a Kondo material are scaled by a single energy parameter, the characteristic temperature T_0 .^{14,15} We thus estimated T_0 using the numerical results of Rajan's and Bicker's approaches as shown in Fig. 1(b). Using Rajan's approach, we presented modeled fits with the angular momenta of $J = 3/2$ ($N = 4$), $J = 5/2$ ($N = 6$), and $J = 7/2$ ($N = 8$). The best fit with smaller misfits is obtained for $N = 6$, implying the lift of the degeneracy due to the crystal electric field (CEF). We note that the inelastic neutron scattering experiments on YbCuAl did not have sufficient evidence to clarify the well-defined CEF splittings,¹⁶ because the CEF splittings and the strength of the Kondo interaction were of a similar order. In addition, the $4f$ -electron contribution to the specific heat C_{4f} showed a maximum at $T \simeq 28$ K with the value $C_{4f} \sim 7 \text{ J mol}^{-1} \text{ K}^{-1}$.¹⁷ Calculated using the Coqblin-Schrieffer model, the peak lies in the value of the maximum specific heat which lies in

between $J = 7/2$ ($C_{\text{max}} = 8.2 \text{ J mol}^{-1} \text{ K}^{-1}$) and $J = 5/2$ ($C_{\text{max}} = 6.2 \text{ J mol}^{-1} \text{ K}^{-1}$).¹⁴ Thus the dominant effect on what in the YbCuAl is the Kondo interaction, although the effect of the CEF likely plays an important role as well. We obtained $T_0 = 93$ K for the Rajan's fits having $J = 5/2$ and 83 K for the Bicker's fit, respectively. These values are comparable to $T_K = 100$ K which was previously estimated using a similar method.¹⁸

B. Lattice constants

The temperature dependencies of the lattice constants and the volume are shown, respectively, in Figs. 1(d) and 1(e), whereas the crystal structure is presented in Fig. 1(c). While the lattice parameters slightly decrease with temperature down to 70 K, they remain almost constant between 70 and 20 K. As shown in Fig. 4(c) below, this anomalous behavior at low temperatures correlates with the change in the Yb valences.

C. Electronic structure

Figure 2(b) shows the Yb $2p$ - $3d$ RXES spectra as a function of the incident photon energy across the Yb L_3 edge at 300 K and 25 GPa for YbCuAl, while PFY-XAS spectra are shown in Fig. 2(a). The Yb valence is nearly trivalent and a small fraction of Yb^{2+} is present in the spectra. Energy transfer in Fig. 2(b) is defined as the difference between the incident and emitted photon energies. The Raman component of the RXES spectrum is clearly observed in the double peaks which remain at constant transferred energies below the absorption edge at $h\nu \sim 8944$ eV, corresponding to the Yb^{2+} ($4f^{13}$) and Yb^{3+} ($4f^{14}$) configurations. The PFY-XAS peak at $h\nu = 8935$ eV may correspond to the quadrupole (QP) transition,⁵ that is insensitive to changes in temperature or pressure in our measurements. Above the absorption edge,

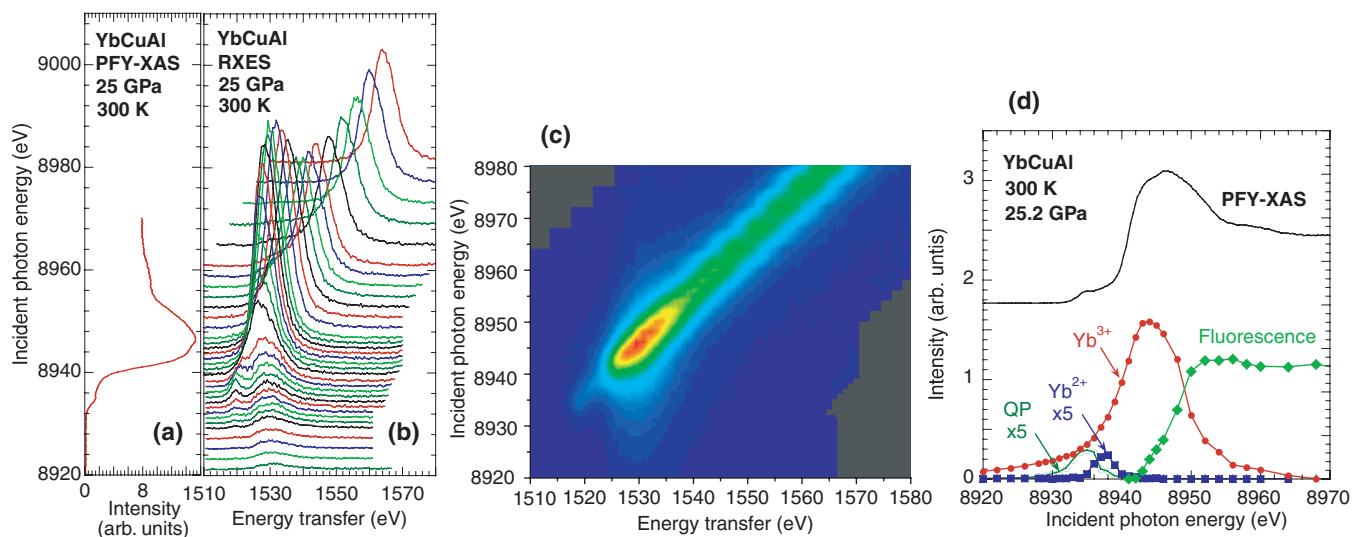


FIG. 2. (Color online) $2p$ - $3d$ RXES spectra of YbCuAl at (a) 25 GPa and 300 K, and (b) as a function of the incident photon energies with the corresponding PFY-XAS spectrum. Vertical offset of the RXES spectra in (b) has been scaled to the incident energy axis of the PFY-XAS spectra in (a). Contour images of the RXES spectra are shown in (c). Raman and fluorescence components (d) as a function of the incident energy dependent intensity of the Yb^{2+} and Yb^{3+} are inferred from fitting the RXES spectra with the PFY-XAS spectra. In (d) the intensities of quadrupole and f^2 components are multiplied by a factor of 5.

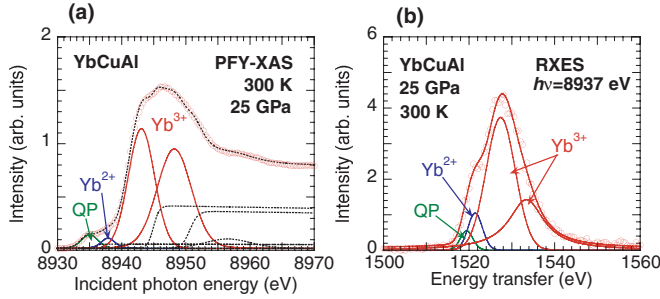


FIG. 3. (Color online) (a) PFY-XAS spectrum at 300 K and 25 GPa. (b) RXES spectrum at the incident photon energy of $h\nu = 8937$ eV. Examples of the fit to the PFY-XAS and RXES spectra are also shown (solid lines).

the energy transfer of the fluorescence peaks changes linearly with the incident energy. These trends are also visible in the two-dimensional contour maps in Fig. 2(c).

Examples of the fitting results for the PFY-XAS spectrum at 25 GPa and 300 K and the RXES spectrum at $h\nu = 8937$ eV are shown in Fig. 3. We fitted the PFY-XAS and RXES spectra with Voigt functions assuming three components of Yb^{2+} ($4f^{13}$), Yb^{3+} ($4f^{14}$), and fluorescence with the QP component. A proper fit of the Yb^{3+} feature required use of two components. The split of the Yb^{3+} component arises from the splitted $5d$ band above the Fermi level.^{19,20} In YbInCu_4 and related compounds, we observed a similar split of the Yb^{3+} component that was previously noted.²¹ This spectrum has been well reproduced theoretically in YbInCu_5 by assuming two semielliptic DOS of the $5d$ band.²² These results indicate that the split of the Yb^{3+} component is mainly due to the nature of the $5d$ band. Furthermore, the PFY-XAS and RXES spectra reflect the final state effect, but do not involve the ground state directly.²³ However, the spectra for Yb_2O_3 displayed the Yb^{3+} peak around 8948 eV, while no evidence of a Yb^{4+} ($4f^{12}$) related feature caused by the final state effect was observed.²⁴ We note that the Yb valence estimated from our results agrees well with the values obtained by other methods as described below. This evidence suggests that the final-state effects are, if existing at all, very weak.

The fitting results of the RXES spectra as a function of the incident photon energy in Fig. 2(b) are summarized in Fig. 2(d) along with a PFY-XAS spectrum. The fits enable us to confirm the presence of the quadrupole, fluorescence, and two Raman components, and to track their energy-dependent intensities. The estimated Yb valence ν from the fit for the Raman components in Fig. 2(d) is 2.98 ± 0.01 at 25 GPa, which is almost the same as the value derived from the fit to the PFY-XAS spectrum at 25 GPa (see further discussion below).

The temperature dependence of the PFY-XAS spectra at ambient pressure is shown in Fig. 4(a). Figure 4(b) shows the temperature-dependent RXES spectra measured at the Yb^{2+} resonance energy of $h\nu = 8938$ eV. Figure 4(c) shows the temperature dependence of the Yb valence estimated from the fit for the PFY-XAS spectra. Temperature dependence of the Yb valence derived from the fit of the RXES spectra after the normalization with the absolute values derived from PFY-XAS is also shown in the Fig. 4(c). The trends of the Yb valence obtained from both spectra are similar, which further substanti-

ates the reliability of our analytical method. The estimated Yb valence of 2.96 ± 0.01 at 300 K and ambient pressure is close to the previously reported values of 2.94 (Ref. 18) from the SIAM fit to the susceptibility and 2.95 (Ref. 25) at ambient pressures. A characteristic temperature of $T_0 = 90$ K and a bandwidth of $\Gamma = 60$ meV were derived from Mössbauer spectroscopic results.²⁶ From the relation $n_f/(1 - n_f) = (2J + 1)\Gamma/(\pi T_0)$ (n_f is $4f$ fractional occupancy), the result was $\nu = 2.96$, which is the same value to our estimate.

The Yb valence decreases with decreasing temperature and the most notable change in the valence occurs below 100 K. The temperature dependence of the valence is expressed as the following equation based on the SIAM with the noncrossing approximation:¹⁵ $\nu(T) = 2 + n_f(\infty) - [\Delta n_f(T)/\Delta n_f(0)]\Delta n_f(0)$, where $n_f(\infty)$ and $\Delta n_f(T)$ are the intermediate temperature limit of the valence and the decrease in the total valence, respectively. We used a universal curve for $\Delta n_f(T)/\Delta n_f(0)$ as a function of the normalized temperature T/T_0 in Fig. 14 of Ref. 15. In the analyses we derived the bandwidth (D) from the electronic specific coefficient to obtain $n_f(\infty)$ using $\gamma = 5$ mJ mol⁻¹ K⁻² for LuCuAl .¹⁷ D and $n_f(\infty)$ are estimated to be approximately 3.1 eV and 0.97, respectively. The temperature dependence of the valence was obtained from fitting the PFY-XAS spectra using two fitting methods: (1) The first is with $\Delta n_f(0)$ as a free parameter assuming $T_0 = 93$ K, which is derived from the fit to the susceptibility and (2) the second is with $n_f(\infty)$, $\Delta n_f(0)$, and T_0 as free parameters. The fitted results are shown in Fig. 4(c). The derived value from the first method is slightly higher than the values of the Yb valence obtained experimentally. The derived value from the second method is $T_0 = 159$ K, which is higher than the value previously estimated by Schlottmann.¹⁸ The second model also initializes $n_f(\infty)$ at 0.97, the same value as the first case, showing that reasonable values of the bandwidth can be obtained from these analyses.

Our results in Fig. 4(c) indicate that the temperature-induced valence change is on the order of 1.5% between 300 and 10 K, and that a change of less than 3% occurs down to 0 K. These are in reasonable agreement with a previous estimate based on the difference of the thermal expansion between YbCuAl and LuCuAl , which yielded 3.5% decrease between 300 and 1.5 K.¹⁷ The relatively abrupt decrease of the valence at $T < 100$ K inferred from our measurements indicates an increase of the Kondo effect and the c - f hybridization in this temperature range, which favors the Yb^{2+} state. Whereas a slight thermal contraction of the unit cell is typically expected in materials upon cooling, as shown in Fig. 1(e) the volume of YbCuAl is nearly temperature independent at $T < 100$ K. In YbInCu_4 , a first-order valence transition occurs at 42 K.²⁷⁻²⁹ The change in the Yb valence is on the order of 0.1 (Ref. 30) and the corresponding volume change is approximately 0.5%.³¹ In YbCuAl , on the other hand, the change in the volume is approximately 0.3% between 20 and 300 K, while the change in the valence is approximately 0.05. Thus, the rate of the volume change roughly corresponds to that of the Yb valence. Our results for YbCuAl interestingly suggest that the effects from the thermal contraction of the unit cell and the increase in the c - f hybridization and thus the Yb valence compensate each other at temperatures between 20 to 80 K.

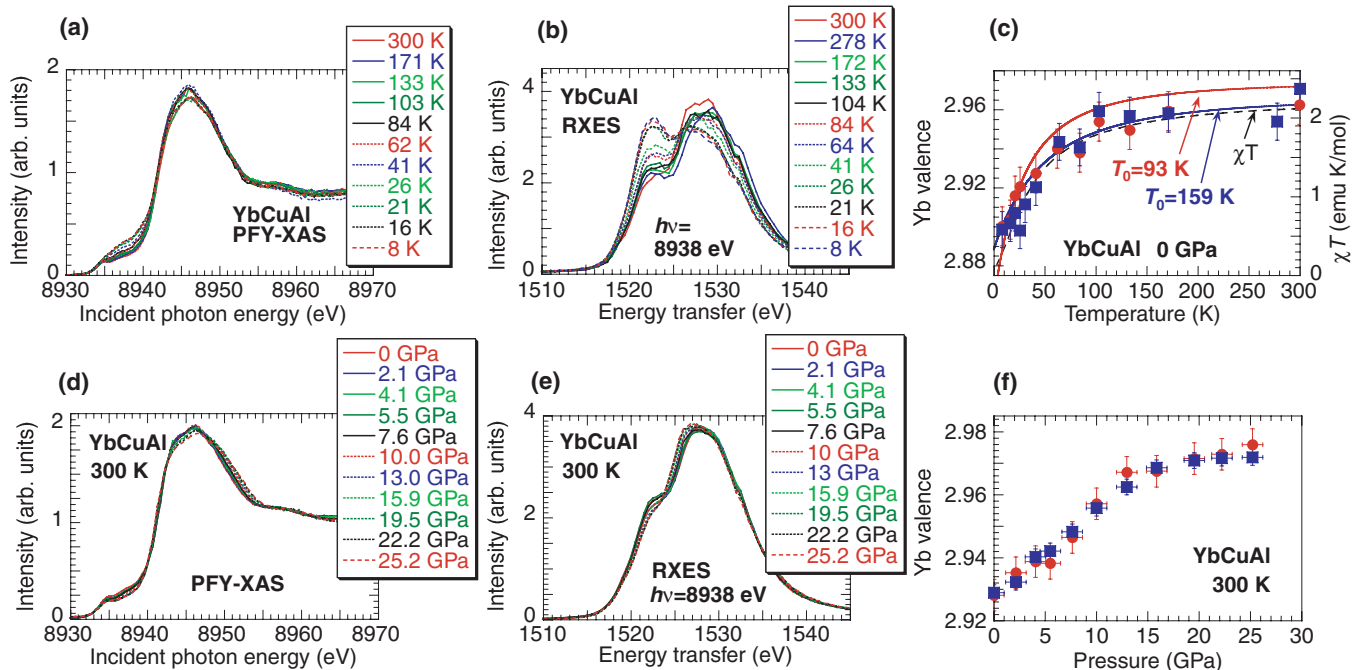


FIG. 4. (Color online) Temperature or pressure dependence PFY-XAS and RXES spectra of YbCuAl at ambient pressure. (a) PFY-XAS spectra of YbCuAl at ambient pressure. (b) RXES spectra. (c) Yb valence estimated from the fit to the PFY-XAS spectra (closed circles). The Yb valence obtained from the RXES spectra in (b) (closed squares) is also shown. These values are scaled with those from the PFY-XAS spectra for comparison. Fitted curves based on the SIAM for the Yb valence are shown with the χT curve (long-dashed line, right vertical axis). (d) Pressure dependence of the PFY-XAS spectra at 300 K. (e) Pressure dependence of the the RXES spectra. (f) Pressure dependent Yb valence (closed circles) estimated from the fit to the PFY-XAS spectra. The Yb valence obtained from the RXES spectra in (e) (closed squares) is also shown. These values in (c) and (f) are corrected to those from the PFY-XAS spectra.

We also measured the PFY-XAS spectra and the RXES spectra at $h\nu = 8938$ eV as a function of pressure at 300 K, respectively shown in Figs. 4(d) and 4(e). The pressure dependence of the Yb valence up to 25 GPa is shown in Fig. 4(f). The mean value of ν at ambient pressure and room temperature is slightly different in Figs. 4(c) and 4(f), suggesting that the absolute value of ν depends on the sample or experimental conditions, including the sample environments inside or outside of the high-pressure cell. However, with the relative changes in the valence within each data set, temperature and pressure are unaffected and should remain robust. We note that at first glance, pressure-induced changes in the line shapes of the PFY-XAS and RXES data seem small, whereas the amplitude of pressure and temperature-induced valence variations, as estimated from the fits, is comparable [cf. Figs. 4(c) and 4(f)]. Under pressure, these spectral bands become broadened, resulting in larger spectral features, and also weaker maximum intensities for constant peak areas. This causes a smearing out of the apparent pressure-induced line shape changes. For example, band broadening and valence increase under pressure result in a decrease and an increase of the Yb^{3+} peak maximum, respectively, which explains the little variation of the experimental peak intensity. The Yb^{3+} band broadening also obscures the pressure-induced change in the intensity of the Yb^{2+} component. As seen in Fig. 4(f), there is a steady, monotonous increase of the valence up to ~ 13 GPa, although the valence increase is markedly milder with further pressure increase. Even at the maximum pressure of 25 GPa in our study, Yb does not exhibit a purely trivalent

state. This is at odds with a previous Mössbauer study which suggested that the trivalency is completed at 5 GPa,⁷ showing that the accuracy and reliability of valence estimates based on L -edge x-ray spectroscopic measurements of the lanthanide compounds remain to be resolved. Furthermore, given that the onset pressure of the magnetic order is $P_m = 8$ GPa,⁸ our results imply that Yb already begins to behave as a magnetic trivalent ion before reaching a pure trivalent state at ~ 2.95 .

IV. DISCUSSION

The pressure dependence of the physical properties of YbCuAl is reminiscent to that in YbCu_2Si_2 (Ref. 32) and YbInAu_2 (Ref. 8). In YbCu_2Si_2 we also note that the magnetic order also sets in at $P_m = 8$ GPa.³³ A change in the slope of the pressure-dependent valence occurs at 11 GPa and 300 K and at 9 GPa and 7 K, beyond which the pressure effect is much less significant.⁵ Interestingly, the changes at 9 and 11 GPa pressures are just above P_m . Our results also show a clear change in the slope of the pressure-dependent valence for YbCuAl at approximately 13 GPa and 300 K. Based on the analogy with YbCu_2Si_2 ,⁵ it is conceivable that the change in the slope of pressure-dependent Yb valence in YbCuAl reduces by about 2 GPa at low temperatures. This transition pressure is also slightly above the onset pressure for the magnetic order.⁸

The temperature-dependent resistivity revealed Fermi liquid behavior of YbCuAl occurs at approximately 8 GPa.⁸ Although clear evidence for the quantum criticality has not yet

been observed for YbCuAl up to 8 GPa, it is generally expected that intersite magnetic fluctuations are enhanced around the magnetic instability point and likely play an important role in the thermodynamical properties of the system. Thus, the change in the slope of the valence increase may suggest that valence fluctuations in YbCuAl, as in YbCu₂Si₂, are somewhat connected to the magnetic fluctuations induced in the vicinity of the magnetic instability point. Consequently, this also raises the possibility that the flattening in the pressure-dependent valence is a general characteristic nature of the intermediate-valence rare-earth systems at P - T conditions close to their cross out magnetic instability points. This calls for additional investigation on the T^2 dependence at higher pressures in the YbCuAl system in order to confirm the existence of the QCP. We note that in YbRh₂Si₂, the QCP was previously confirmed using the divergent character of C/T ,³⁴ where C is specific heat, although the T^2 dependence of the resistivity was observed at the QCP. Therefore, *in situ* observation of the divergence of C/T would provide sufficient experimental evidence to confirm the occurrence of the QCP.

Here we further discuss another perception for the change in the slope of the valence-pressure curve as a possible indication of the transition from the intermediate-valence (IV) regime to the Kondo regime. In the IV regime, the effect of CEF is obscured because of the high Kondo temperature, while in the Kondo regime, T_K is lower than CEF; thereby, a well-defined CEF splitting should be observed at P - T conditions in the system. This transition has indeed been observed in YbNi₂Ge₂. It has been reported that the temperature dependence of the electrical resistivity of YbNi₂Ge₂ displays a single maximum related to the Kondo effect for pressures below 3.4 GPa, while two maxima are developed at pressures above 3.4 GPa.³⁵ This is suggestive of a transition from the IV to the Kondo regime. Indeed, we have observed an inflection in the valence-pressure curve at approximately 5 GPa and room temperature.¹¹ Furthermore, from the pressure-dependent resistivity data, it has been suggested that the ratio A/γ^2 , known as the Kadowaki-Woods ratio,³⁶ increases by nearly two orders of magnitude. This increase in the Kadowaki-Woods ratio is in accordance with the decrease of the ground state degeneracy N due to the CEF effect as T_K is reduced by pressure.³⁷ Therefore, the change in the slope of the pressure-dependent valence possibly indicates the transition from the IV to the Kondo regime. This transition is accompanied by the reduction of the ground state degeneracy and a rapid decrease of T_K , resulting in the magnetic ordering at low temperature.

The volume contraction of what system in temperature cooling favors the magnetic ground state of the Yb³⁺ ion because of its smaller ionic radius compared with the Yb²⁺ ion. The pressure-induced volume contraction at applied pressures up to 10 GPa is typically about one order magnitude larger than in temperature cooling. Our results show that a volume contraction of about 1% occurs with decreasing temperature from 300 to 20 K, corresponding to the application of external pressure slightly less than 1 GPa. At ambient pressure, the c - f hybridization is enhanced by cooling at temperatures below the characteristic temperature of approximately 100 K, resulting in the increase of the Yb²⁺ state which compensates the volume contraction effect.

We finally address the absence of the reentrance into the mixed-valence state within the pressure range of the present study. As stated in the Introduction, the electrical resistivity of YbCuAl at room temperature shows a minimum at 8 GPa, while the electrical resistivity increases with pressure at above 8 GPa. From our results, the possibility for an increase in T_K at pressures above 8 GPa is unlikely, ruling out the scenario proposed by Goltsev and Abd-Elmeguid,⁴ because the Yb valence constantly enhances at applied pressures. Based on this evidence, we would argue that the increase of ρ at pressures above 8 GPa results from the enhancement in electron scattering due to the increase of the magnetic local moment of the Yb³⁺ ion. We also note that in YbCuAl and YbCu₂Si₂, the CEF effect can significantly influence their physical properties even at ambient pressure.^{16,38} Although inelastic neutron scattering experiments did not reveal a well-defined CEF excitation, the best fit to our magnetic susceptibility result can be obtained using Rajan's model, taking into account the degeneracy, indicating that the CEF at ambient pressure can have a similar order of effects on T_K . The anomalous behavior of the resistivity in YbCuAl and YbCu₂Si₂ at high pressures had been previously attributed to the CEF effect and the RKKY interaction.³⁹ Applied pressure induces a further increase in the CEF and the CEF effects such that they become more apparent with respect to the Kondo effect,⁴⁰ thereby making the reentrance of the valence transition improbable. Other Yb systems such as cubic YbCu₅ and related compounds should be favorable candidates for reentrant valence transitions because the CEF effect seems to play an insignificant role in these cubic compounds.⁴¹

V. CONCLUSION

Temperature- and pressure-induced changes in the electronic structure of the heavy fermion compound YbCuAl have been measured using PFY-XAS and RXES at temperatures below 8 K and ambient pressure, and at pressures up to 25 GPa and room temperature. The temperature dependence of the Yb valence is well represented within the SIAM and we have obtained a characteristic temperature comparable to the previous evaluations of the Kondo temperature obtained from the magnetic susceptibility measurements. Our results suggest that the thermal contraction is compensated for by the volume increase caused by enhancement of the c - f hybridization at low temperature due to the Kondo effect. Our pressure-dependent results reveal a continuous increase of the Yb valence up to 25 GPa, with a decrease of the slope around 13 GPa. The proximity of this change in the slope to the magnetic instability confirms the interplay between electronic and magnetic fluctuations. The change in the slope of the pressure-dependent valence data can likely be associated with the transition from the intermediate valence state with no CEF effect to the Kondo regime where CEF effect overcomes T_K . As a result, the RKKY interaction dominates the low-temperature properties. Such interplay has already been suggested to occur in YbNi₂Ge₂ and YbCu₂Si₂ under pressure, suggesting that this may be an intrinsic nature in all trivalent Yb-bearing systems. A better fit to the magnetic susceptibility is obtained using Rajan's model, taking into

account the degeneracy, indicating the presence of CEF effects even at ambient pressure. Since the reentrance of the valence transition was not observed at high pressure, the anomaly in the pressure-dependent resistivity may arise from the increased local magnetic moment of Yb^{3+} as well as the CEF effect.

ACKNOWLEDGMENTS

The experiments were performed at SPring-8 Taiwan beamline BL12XU under SPring-8 Proposals No. 2011B4260

and No. 2012B4625 and corresponding NSRRC Proposals No. 2011-2-021-2 and No. 2011-2-021-4. This work is partly supported by Grants in Aid for Scientific research (KAKENHI Kiban C No. 22540343 and No. 23540411) from the Japan Society for the Promotion of Science. This work at UT Austin was supported as part of EFree, an Energy Frontier Research Center funded by the US Department of Energy Office of Science, Office of Basic Energy Sciences under Award DE-SC0001057. The authors thank B. Shalab and L. Dafov for editing the manuscript.

- ¹J. M. Lawrence, P. S. Riseborough, and R. D. Parks, *Rep. Prog. Phys.* **44**, 1 (1981).
- ²G. R. Stewart, *Rev. Mod. Phys.* **73**, 797 (2001); **78**, 743 (2006).
- ³H. v. Löhneysen, A. Rosch, M. Vojta, and P. Wölfle, *Rev. Mod. Phys.* **79**, 1015 (2007).
- ⁴A. V. Goltsev and M. M. Abd-Elmeguid, *J. Phys. C: Condens. Matter* **17**, S813 (2005).
- ⁵A. Fernandez-Pañella, V. Balédent, D. Braithwaite, L. Paolasini, R. Verbeni, G. Lapertot, and J.-P. Rueff, *Phys. Rev. B* **86**, 125104 (2012).
- ⁶J. M. Mignot and J. Wittig, *Physics of Solid Under High Pressure*, edited by J. S. Schilling and R. N. Shelton (North-Holland, Amsterdam, 1981), p. 311.
- ⁷M. Schöppner, J. Moser, A. Kratzer, U. Potzel, J. M. Mignot, and G. M. Kalvius, *Z. Phys. B* **63**, 25 (1986).
- ⁸K. Alami-Yadri, H. Wilhelm, and D. Jaccard, *Solid State Commun.* **108**, 279 (1998).
- ⁹T. Jeong, *Physica B* **390**, 309 (2007).
- ¹⁰H. Yamaoka, I. Jarrige, N. Tsujii, N. Hiraoka, H. Ishii, and K.-D. Tsuei, *Phys. Rev. B* **80**, 035120 (2009).
- ¹¹H. Yamaoka, I. Jarrige, N. Tsujii, J.-F. Lin, N. Hiraoka, H. Ishii, and K.-D. Tsuei, *Phys. Rev. B* **82**, 035111 (2010).
- ¹²H. Yamaoka, I. Jarrige, N. Tsujii, M. Imai, J.-F. Lin, M. Matsunami, R. Eguchi, M. Arita, K. Shimada, H. Namatame, M. Taniguchi, M. Taguchi, Y. Senba, H. Ohashi, N. Hiraoka, H. Ishii, and K.-D. Tsuei, *Phys. Rev. B* **83**, 104525 (2011).
- ¹³H. Yamaoka, I. Jarrige, N. Tsujii, J.-F. Lin, T. Ikeno, Y. Isikawa, K. Nishimura, R. Higashinaka, H. Sato, N. Hiraoka, H. Ishii, and K.-D. Tsuei, *Phys. Rev. Lett.* **107**, 177203 (2011).
- ¹⁴V. T. Rajan, *Phys. Rev. Lett.* **51**, 308 (1983).
- ¹⁵N. E. Bickers, D. L. Cox, and J. W. Wilkins, *Phys. Rev. B* **36**, 2036 (1987).
- ¹⁶A. P. Murani, W. C. M. Mattens, F. R. de Boer, and G. H. Lander, *Phys. Rev. B* **31**, 52 (1985).
- ¹⁷R. Pott, R. Scheffzyk, and D. Wohlleben, *Z. Phys. B* **44**, 17 (1981).
- ¹⁸P. Schlottmann, *Z. Phys. B* **57**, 23 (1984).
- ¹⁹K. Takegahara and T. Kasuya, *J. Phys. Soc. Jpn.* **59**, 3299 (1990).
- ²⁰V. N. Antonov, B. N. Harmon, and A. N. Yaresko, *Phys. Rev. B* **66**, 165209 (2002).
- ²¹H. Yamaoka, N. Tsujii, K. Yamamoto, A. M. Vlaicu, H. Ohashi, H. Yoshikawa, T. Tochio, Y. Ito, A. Chainani, and S. Shin, *Phys. Rev. B* **78**, 045127 (2008).
- ²²A. Kotani, *Eur. Phys. J. B* **85**, 31 (2012).
- ²³H. Yamaoka, Y. Zekko, A. Kotani, I. Jarrige, N. Tsujii, J.-F. Lin, J. Mizuki, H. Abe, H. Kitazawa, N. Hiraoka, H. Ishii, and K.-D. Tsuei, *Phys. Rev. B* **86**, 235131 (2012).
- ²⁴K. Yamamoto, H. Yamaoka, N. Tsujii, A. M. Vlaicu, H. Ohashi, S. Sakakura, T. Tochio, Y. Ito, A. Chainani, and S. Shin, *J. Phys. Soc. Jpn.* **76**, 124705 (2007).
- ²⁵K. R. Bauschpiess, W. Boksich, E. Holland-Moritz, H. Launois, R. Pott, and D. Wohlleben, *Valence Fluctuation in Solids*, edited by L. M. Falicov, W. Hanle, and M. B. Maple (North-Holland, Amsterdam, 1981), p. 417.
- ²⁶P. Bonville, J. A. Hodges, P. Imbert, D. Jaccard, J. Sierro, M. J. Besnus, and A. Meyer, *Physica B* **163**, 347 (1990).
- ²⁷I. Felner and I. Nowik, *Phys. Rev. B* **33**, 617 (1986).
- ²⁸I. Felner, I. Nowik, D. Vaknin, U. Potzel, J. Moser, G. M. Kalvius, G. Wortmann, G. Schmiester, G. Hilscher, E. Gratz, C. Schmitzer, N. Pillmayr, K. G. Prasad, H. de Waard, and H. Pinto, *Phys. Rev. B* **35**, 6956 (1987).
- ²⁹K. Kojima, H. Hayashi, A. Minami, Y. Kasamatsu, and T. Hihara, *J. Magn. Magn. Mater.* **81**, 267 (1989).
- ³⁰H. Sato, K. Shimada, M. Arita, K. Hiraoka, K. Kojima, Y. Takeda, K. Yoshikawa, M. Sawada, M. Nakatake, H. Namatame, M. Taniguchi, Y. Takata, E. Ikenaga, S. Shin, K. Kobayashi, K. Tamasaku, Y. Nishino, D. Miwa, M. Yabashi, and T. Ishikawa, *Phys. Rev. Lett.* **93**, 246404 (2004).
- ³¹V. N. Lazukov, A. S. Ivanov, F. Ritter, P. A. Alekseev, W. Assmus, I. P. Sadikov, and N. N. Tiden, *Physica B* **350**, E139 (2004).
- ³²H. Winkelmann, M. M. Abd-Elmeguid, H. Micklitz, J. P. Sanchez, P. Vulliet, K. Alami-Yadri, and D. Jaccard, *Phys. Rev. B* **60**, 3324 (1999).
- ³³A. Fernandez-Pañella, D. Braithwaite, B. Salce, G. Lapertot, and J. Flouquet, *Phys. Rev. B* **84**, 134416 (2011).
- ³⁴G. Knebel, R. Boursier, E. Hassinger, G. Lapertot, P. G. Niklowitz, A. Pourret, B. Salce, J. P. Sanchez, I. Sheikin, P. Bonville, H. Harima, and J. Flouquet, *J. Phys. Soc. Jpn.* **75**, 114709 (2006).
- ³⁵G. Knebel, D. Braithwaite, G. Lapertot, P. C. Canfield, and J. Flouquet, *J. Phys.: Condens. Matter* **13**, 10935 (2001).
- ³⁶K. Kadowaki and S. B. Woods, *Solid State Commun.* **58**, 507 (1986).
- ³⁷N. Tsujii, H. Kontani, and K. Yoshimura, *Phys. Rev. Lett.* **94**, 057201 (2005).
- ³⁸E. Holland-Moritz, D. Wohlleben, and M. Loewenhaupt, *Phys. Rev. B* **25**, 7482 (1982).
- ³⁹K. Alami-Yadri, H. Wilhelm, and D. Jaccard, *Physica B* **259–261**, 157 (1999).
- ⁴⁰P. Bonville, E. Vincent, and E. Bauer, *Eur. Phys. J. B* **8**, 363 (1999).
- ⁴¹H. Michor, K. Kreiner, N. Tsujii, K. Yoshimura, K. Kosuge, and G. Hilscher, *Physica B* **319**, 277 (2002).